Cell. Mol. Life Sci. (2017) 74:543–554
DOI 10.1007/s00018-016-2355-2

Cellular and Molecular Life Sciences

ORIGINAL ARTICLE

Death receptor 3 mediates necroptotic cell death

Sebastian Bittner[1] · **Gertrud Knoll**[1] · **Martin Ehrenschwender**[1]

Received: 15 April 2016 / Revised: 9 August 2016 / Accepted: 31 August 2016 / Published online: 3 September 2016

Abstract Death receptor 3 (DR3) was initially identified as a T cell co-stimulatory and pro-inflammatory molecule, but further studies revealed a more complex role of DR3 and its ligand TL1A. Although being a death receptor, DR3 gained to date predominantly attention as a contributor to inflammation-driven diseases. In our study, we investigated the cell death pathways associated with DR3. We show that in addition to apoptosis, DR3 can robustly trigger necroptotic cell death and provide evidence for TL1A-induced, DR3-mediated necrosome assembly. DR3-mediated necroptosis critically depends on receptor-interacting protein 1 (RIP1) and RIP3, the core components of the necroptotic machinery, which activate the pseudo-kinase mixed lineage kinase domain-like, the prototypic downstream effector molecule of necroptosis. Moreover, we demonstrate that DR3-mediated necroptotic cell death is accompanied by, but does not depend on generation of reactive oxygen species. In sum, we identify DR3 as a novel necroptosis-inducing death receptor and thereby lay ground for elucidating the (patho-) physiological relevance of DR3-mediated necroptotic cell death in vitro and in vivo.

Keywords Death receptor 3 · Necroptosis · TL1A · RIP3 · MLKL · TNFRSF25

✉ Martin Ehrenschwender
martin.ehrenschwender@ukr.de

[1] Institute of Clinical Microbiology and Hygiene, University Hospital Regensburg, Franz-Josef-Strauss-Allee 11, 93053 Regensburg, Germany

Introduction

Regulation of cell death is critical for tissue homeostasis and dysregulation contributes to numerous pathologies [1, 2]. Death receptors constitute a subgroup of the tumor necrosis factor (TNF) receptor superfamily (TNFRSF) and have been functionally linked to two cell death modalities: apoptosis and necroptosis. Apoptotic cell death is orchestrated through the activation of caspases and has distinct morphological features including membrane blebbing, cell shrinkage and nuclear fragmentation [3, 4]. In contrast, necroptosis (or programmed necrosis) occurs in a caspase-independent fashion and also highlights a different morphological signature with cell swelling, membrane rupture and release of intracellular contents [5–7]. Initiation of both, apoptotic and necroptotic cell death has been described for the death receptors TNF-related apoptosis-inducing ligand receptor 1 (TRAILR1), TRAILR2, CD95 and TNF-receptor 1 (TNFR1) [8, 9]. Extensive studies of the latter led to insights into the molecular mechanisms of apoptosis and necroptosis. Binding of TNF to TNFR1 triggers recruitment of receptor-interacting protein-1 (RIP1), TNFR1-associated death domain (TRADD), cellular inhibitor of apoptosis protein 1 (cIAP1), cIAP2 and TNFR-associated factor 2 (TRAF2), together forming complex I [10]. RIP1 functions as molecular switch between survival and cell death. On the one hand, RIP1 stabilizes cellular FADD-like IL-1β-converting enzyme-inhibitory protein (cFLIP) levels and (following cIAP1/2-mediated ubiquitination) triggers NF-κB-mediated induction of anti-apoptotic genes, both protecting cells against TNF-induced cytotoxicity [11–14]. On the other hand, ubiquitin-dependent phosphorylation of RIP1 controls its dissociation from the plasma membrane and interaction with FADD, RIP3, $cFLIP_L$ and pro-caspase-8, forming the

death-inducing complex IIb [10, 12, 15–17]. Within complex IIb, caspase-8 activity is decisive for subsequent apoptotic or necroptotic cell death. Caspase-8 not only cleaves, and thereby activates downstream effector caspases to initiate the execution phase of apoptosis, but also blocks necroptosis by cleaving RIP1 and RIP3, the core components of the necroptotic machinery. This anti-necroptotic function of caspase-8 is physiologically counteracted by the pseudo-caspase $cFLIP_L$ or can be pharmacologically blocked by zVAD-fmk. Lack of caspase-8 activity enables RIP1 and RIP3 to interact through their RIP homotypic interacting motif (RHIM) domains and to phosphorylate each other, thereby forming an amyloid-like structure ("necrosomes") [18]. Necrosome formation critically depends on kinase activity of RIP1 and can be disturbed by necrostatin-1 (Nec-1) [19]. Necroptosis is executed by RIP3-mediated phosphorylation of mixed linage kinase domain-like (MLKL) [20–23], resulting in MLKL oligomerization, translocation to the cell membrane and finally membrane rupture [24]. The MLKL-targeting molecule necrosulfonamide (NSA) efficiently blocks necroptosis downstream of RIP3 activation [21]. Death receptor 3 (DR3, also known as TNFRSF25) was initially identified as a T cell co-stimulatory molecule [25] and suggested to be closely related to TNFR1. Binding of its cognate ligand TL1A causes a predominantly pro-inflammatory cellular response [26]. However, DR3 is also capable of inducing apoptosis and we recently demonstrated that mimetics of the second mitochondria-derived activator of caspase (SMAC mimetics) boost DR3-mediated cell death induction [27–29]. Whether DR3 is capable to initiate necroptosis has to date not been addressed.

Here we show that when caspase activation is blocked, DR3 activation can trigger a cell death modality that involves RIP1 and RIP3. Mechanistically, we provide evidence for TL1A-induced, DR3-mediated necrosome formation with subsequent phosphorylation and oligomerization of the necroptosis effector MLKL, thus establishing DR3 as a novel necroptosis-inducing death receptor.

Materials and methods

Cells, antibodies and reagents

TF-1 and L929 cells were obtained from the German Collection of Microorganisms and Cell Cultures (Braunschweig, Germany). Ku812F cells were purchased from LGC Standards GmbH (Wesel, Germany). Cell lines were grown in RPMI 1640 medium (PAN Biotech, Aidenbach, Germany) supplemented with 10 % (v/v) fetal calf serum (Sigma, Steinheim, Germany). Medium for TF-1 cells was additionally supplemented with 5 ng/mL human GM-CSF (Immunotools, Friesoythe, Germany). Antibodies used in the study: cIAP1, cIAP2, RIP3, caspase-8, caspase-3 (Cell Signaling, Beverly, MA, USA); DR3 and RIP1 (R&D Systems, Wiesbaden, Germany); tubulin: Dunnlab (Asbach, Germany); MLKL and phospho-MLKL (EMD Millipore, Temecula, California, USA). Chemicals: MTT (3-[4,5-dimethylthiazol-2-yl]-2,5-diphenyl tetrazolium bromide), cycloheximide (CHX) and TAK1 inhibitor (5Z)-7-oxozeaenol (TAK1i): Biomol (Hamburg, Germany); zVAD-fmk (carbobenzoxy-valyl-alanyl-aspartyl-[*O*-methyl]-fluoromethylketone): Bachem (Bubendorf, Switzerland); BV6 and 17-AAG: Selleck Chemicals (Houston, TX, USA). Necrosulfonamide (NSA): Tocris Bioscience (Bristol, UK); Necrostatin-1 (Nec-1): Stress-Marq (Victoria, Canada); 7-Cl-O-Nec1 (Nec1s): Tebu-bio GmbH (Offenbach, Germany); GSK'872: Merck (Darmstadt, Germany); 7-AAD (R&D Systems); butylated hydroxyanisole (BHA): Sigma; human recombinant TNF was provided by D. Männel (University of Regensburg, Germany). Production and purification of FLAG-TNC-TL1A was described previously [29]. Etanercept was obtained from Pfizer (Berlin, Germany).

Cell viability assay

TF-1 (7×10^4 cells/well), Ku812F cells (5×10^4 cells/well) and L929 cells (1×10^4 cells/well) were seeded in 96-well-plates, treated with CHX (2.5 μg/mL) or BV6 (TF-1 10 μM; Ku812F 3 μM; L929 2.5 μM) for 2 h, and subsequently challenged with the indicated concentrations of the ligands in triplicates. Cell viability was determined 4 or 18 h after stimulation using MTT staining (2 h at 37 °C).

Caspase-3/7 activity assay

Caspase activity was measured using the caspase 3/7 activity kit (AAT Bioquest, Sunnyvale, CA, USA) according to manufacturer's instructions in duplicates. Light emission was quantified using a Victor3 Multilabel Reader (Perkin Elmer, Waltham, MA, USA).

Immunoprecipitation

Ku812F cells (1×10^7 per condition) were pre-treated with BV6 (3 μM) and zVAD-fmk (100 μM) for 1 h. Subsequently, cells were stimulated with FLAG-TNC-TL1A (RIP3 and caspase-8 IP 400 ng/mL, FLAG IP 1 μg/mL) for the indicated periods of time. After washing with ice-cold PBS, cell were lysed in MCBL-buffer [NP40 0.5 % (v/v), 150 mM NaCl, 50 mM Tris, pH 7.4] supplemented with complete™ protease inhibitor cocktail (Roche, Mannheim, Germany) for 40 min on ice. Lysates

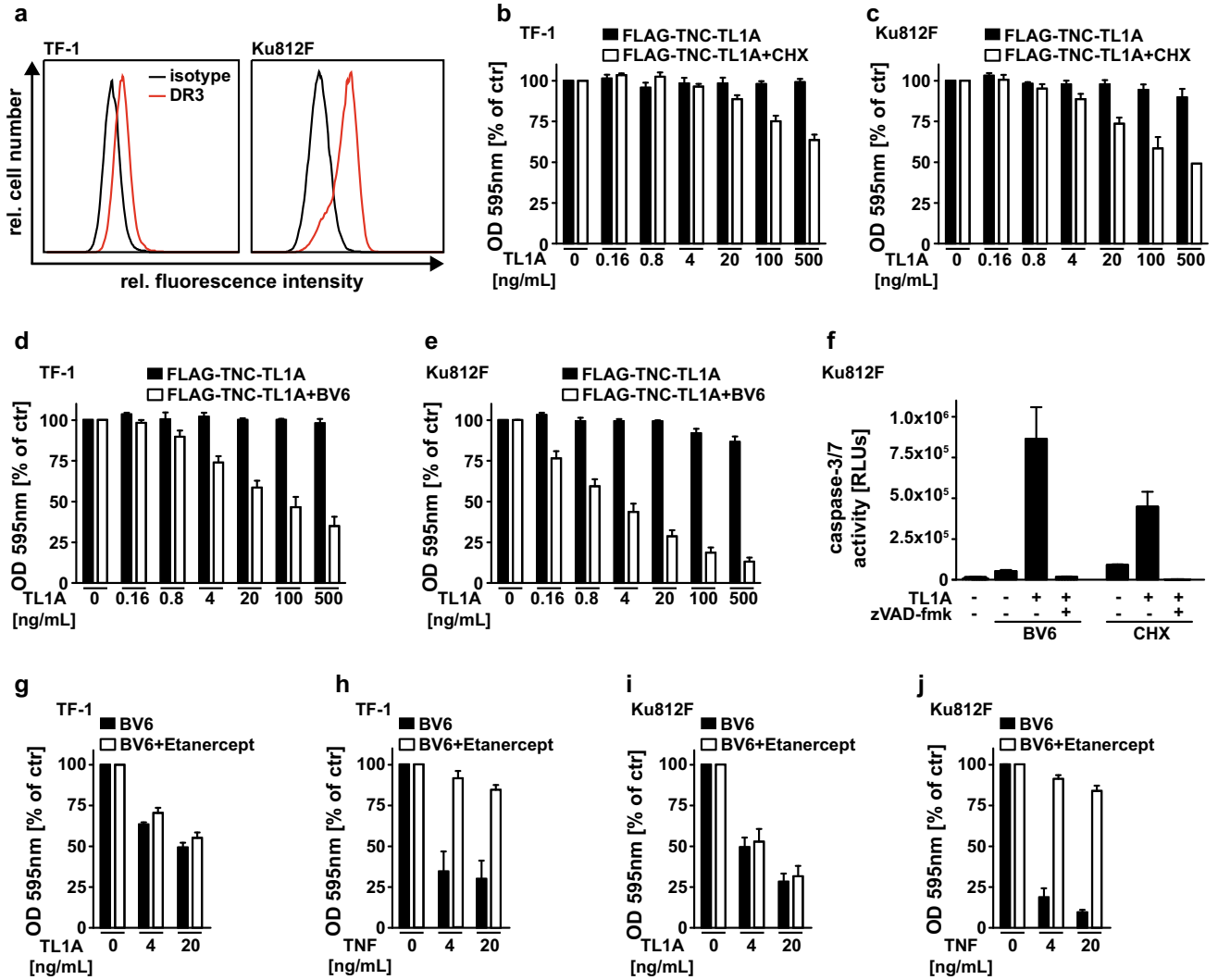

Fig. 1 Depletion of cIAPs enhances DR3-mediated cytotoxicity. **a** Surface expression of DR3 in TF-1 and Ku812F cells was verified by flow cytometry. **b–e** TF-1 and Ku812F cells were treated with cycloheximide (CHX, 2.5 μg/mL) or BV6 (TF-1 10 μM, Ku812F 3 μM) for 2 h, and were subsequently challenged with the indicated concentrations of FLAG-TNC-TL1A for 18 h. Viability was determined by MTT staining. Values are mean ± SEM from three experiments. **f** Ku812F cells were treated with BV6 (3 μM, 2 h), CHX (2.5 μg/mL, 2 h) and/or zVAD-fmk (100 μM, 1 h), and subsequently challenged with FLAG-TNC-TL1A (200 ng/mL). Caspase activity was measured 2.5 h after FLAG-TNC-TL1A addition. Values are mean ± SEM from three experiments. **g–j** TF-1 and Ku812F cells were treated with BV6 (TF-1 10 μM, Ku812F 3 μM) for 2 h, and subsequently challenged with the indicated concentrations of FLAG-TNC-TL1A or TNF in the presence (*white bars*) or absence (*black bars*) of etanercept (1 mg/mL). Viability was determined using MTT staining 18 h after stimulation. Values are mean ± SEM from three experiments. *RLU* relative light units

were cleared by centrifugation (20.000*g*, 20 min, 4 °C) and protein concentration was determined using Pierce BCA Protein Assay Kit (Thermo Scientific, Rockford, USA). 1.5 mg of protein lysate was incubated over night with 2 μg of caspase-8-, RIP3- or 1 μg FLAG-specific antibodies at 4 °C. The next day, antigen–antibody complexes were precipitated using protein G agarose (Roche). After washing in lysis buffer, agarose-bound proteins were eluted by incubation at 95 °C for 10 min in Laemmli sample buffer and analyzed together with the corresponding lysates by Western blotting.

Flow cytometry, ROS detection and 7-AAD staining

DR3 surface expression of Ku812F cells (5×10^5 per group) was measured by staining with DR3-specific, biotinylated antibody (R&D Systems), FITC-conjugated donkey anti-goat (Jackson ImmunoResearch, Baltimore, USA) and Avidin-FITC (R&D Systems). Biotinylated goat IgG (R&D Systems) served as specificity control. Cellular ROS production was quantified after treatment with BV6 (3 μM), zVAD-fmk (100 μM) and the indicated concentrations of TNF ligands. Following staining with

5 μM CM-H_2DCFDA (Invitrogen, Carlsbad, CA, USA) for 30 min at 37° C, Ku812F cells were put on ice and washed twice with ice-cold PBS. Flow cytometry analysis was performed immediately using a FACSCanto flow cytometer (BD Biosciences) following standard procedures. Membrane integrity was measured using 7-AAD staining. In brief, Ku812F cells were treated with BV6 (3 μM, 2 h), zVAD-fmk (100 μM, 1 h) and Nec-1 (100 μM, 1 h), and subsequently challenged with FLAG-TNC-TL1A (200 ng/mL) in triplicates for 4 h. Afterwards, cells were stained with 7-AAD according to manufacturer's instructions (4 °C for 30 min in the dark). 7-AAD incorporation was immediately measured using a FACSCanto flow cytometer (BD Biosciences) following standard procedures.

Western blot analysis

Western blot analysis was essentially performed as described previously [30].

Microscopy

Ku812F cells (4×10^4 cells/well) were seeded in 96-well-plates, treated with BV6 (3 μM, 1 h), zVAD-fmk (100 μM, 1 h), NSA (25 μM, 1 h) and Nec-1 (100 μM, 1 h). Cells were stimulated with FLAG-TNC-TL1A (200 ng/mL) for 3 h and cell morphology was analyzed by bright-field microscopy with a Keyence BZ9000 microscope (Keyence, Osaka, Japan).

siRNA experiments

siRNA oligonucleotides targeting RIPK3 (SMARTpool #M-003534-01) were purchased from Dharmacon (Lafayette, CO, USA). Non-targeting control siRNA was purchased from Qiagen (Hilden, Germany). Briefly, 1.5×10^6 Ku812F cells per condition were washed three times in Opti-MEM®, incubated on ice with 400 pM of siRNA for 5 min. Subsequently, electroporation was performed using a BioRad Gene Pulser Xcell™. Pulse conditions were 300 V, 150 μF and 100 Ω. Knockdown efficacy was assessed after 48 h.

Results

Depletion of cIAPs enhances DR3-mediated cytotoxicity

Despite its predominantly pro-inflammatory nature, DR3 harbors significant cytotoxic potential. In DR3-positive TF-1 and Ku812F cells (Fig. 1a), inhibition of protein translation by cycloheximide (CHX) (Fig. 1b, c) or depletion of cIAP1/2 using the SMAC mimetic BV6 (Fig. 1d, e) allowed TL1A-induced, DR3-mediated cell death. Compared to CHX, BV6 granted a higher rate of TL1A-induced cell death (Fig. 1d, e) concomitant with higher levels of effector caspase-3 and -7 activation (Fig. 1f), indicating ongoing apoptosis. Notably, enhanced cytotoxicity of TL1A in the presence of SMAC mimetics was not attributable to BV6- or TL1A-induced autocrine TNF secretion, as addition of the TNF-neutralizing TNFR2–Fc fusion protein etanercept to TF-1 and Ku812F cells did not impede TL1A-induced cell death (Fig. 1g, i), but expectedly almost completely abrogated TNF-triggered cytotoxicity (Fig. 1h, j).

Fig. 2 Caspase inhibition does not abolish DR3-mediated killing. **a** Ku812F cells were treated with BV6 (3 μM, 2 h) and zVAD-fmk (100 μM, 1 h), and subsequently challenged with FLAG-TNC-TL1A (200 ng/mL) for the indicated periods of time. After washing and lysis, Western blot analysis was performed with antibodies specific for the indicated proteins. Detection of tubulin served as a loading control. **b** Ku812F cells were treated with BV6 (3 μM, 2 h) and zVAD-fmk (100 μM, 1 h), and subsequently challenged with FLAG-TNC-TL1A for 4 h. Viability was determined by MTT staining. Values are mean ± SEM from three experiments. **c** Ku812F cells were treated with BV6 and zVAD-fmk as above in the presence and absence of etanercept (1 mg/mL). Subsequently, cells were challenged with FLAG-TNC-TL1A or TNF for 4 h. Values are mean ± SEM from three experiments. **d** Ku812F cells were treated with BV6 and zVAD-fmk as above, but necrosulfonamide (NSA, 25 μM, *black bars*) or necrostatin-1 (Nec-1, 100 μM, *white bars*) was added 1 h before stimulation with FLAG-TNC-TL1A. Viability was determined by MTT staining. Values are mean ± SEM from three experiments. **e** Ku812F cells were treated with BV6 (3 μM, 2 h), zVAD-fmk (100 μM, 1 h) in the presence and absence of NSA (25 μM, 1 h) or Nec-1 (100 μM, 1 h), and subsequently challenged with FLAG-TNC-TL1A (200 ng/mL). Cell morphology was analyzed 3 h after stimulation by bright-field microscopy. Data shown are representative of two experiments performed. **f** Ku812F cells were treated with BV6 (3 μM, 2 h), zVAD-fmk (100 μM, 1 h) and Nec-1 (100 μM, 1 h), and subsequently challenged with FLAG-TNC-TL1A (200 ng/mL) for 4 h. Loss of membrane integrity was measured by 7-AAD staining using flow cytometry. Values are mean ± SEM from three experiments. **g** Ku812F cells were treated with BV6 (3 μM, 2 h) and zVAD-fmk (100 μM, 1 h) in the presence and absence of Nec-1s (30 μM, 1 h) or GSK'872 (8 μM, 1 h), and subsequently challenged with FLAG-TNC-TL1A. Viability was determined by MTT staining. Values are mean ± SEM from three experiments. **h** Ku812F cells were treated with BV6 (3 μM, 2 h), zVAD-fmk (100 μM,1 h), Nec-1s (30 μM, 1 h) or GSK'872 (8 μM, 1 h), and subsequently challenged with FLAG-TNC-TL1A (200 ng/mL) for 4 h. Loss of membrane integrity was measured by 7-AAD staining using flow cytometry. Values are mean ± SEM from three experiments. **i** Ku812F and TF-1 cells were treated with CHX (2.5 μg/mL) and zVAD-fmk (100 μM) in the presence and absence of Nec-1 (100 μM) for 2 h. Subsequently, cells were challenged with FLAG-TNC-TL1A for 18 h. Viability was determined by MTT staining. Values are mean ± SEM from three experiments

Caspase inhibition does not abolish DR3-mediated killing

Interestingly, activation of effector caspases seemed not to be a *conditio sine qua non* for DR3-mediated cell death. In

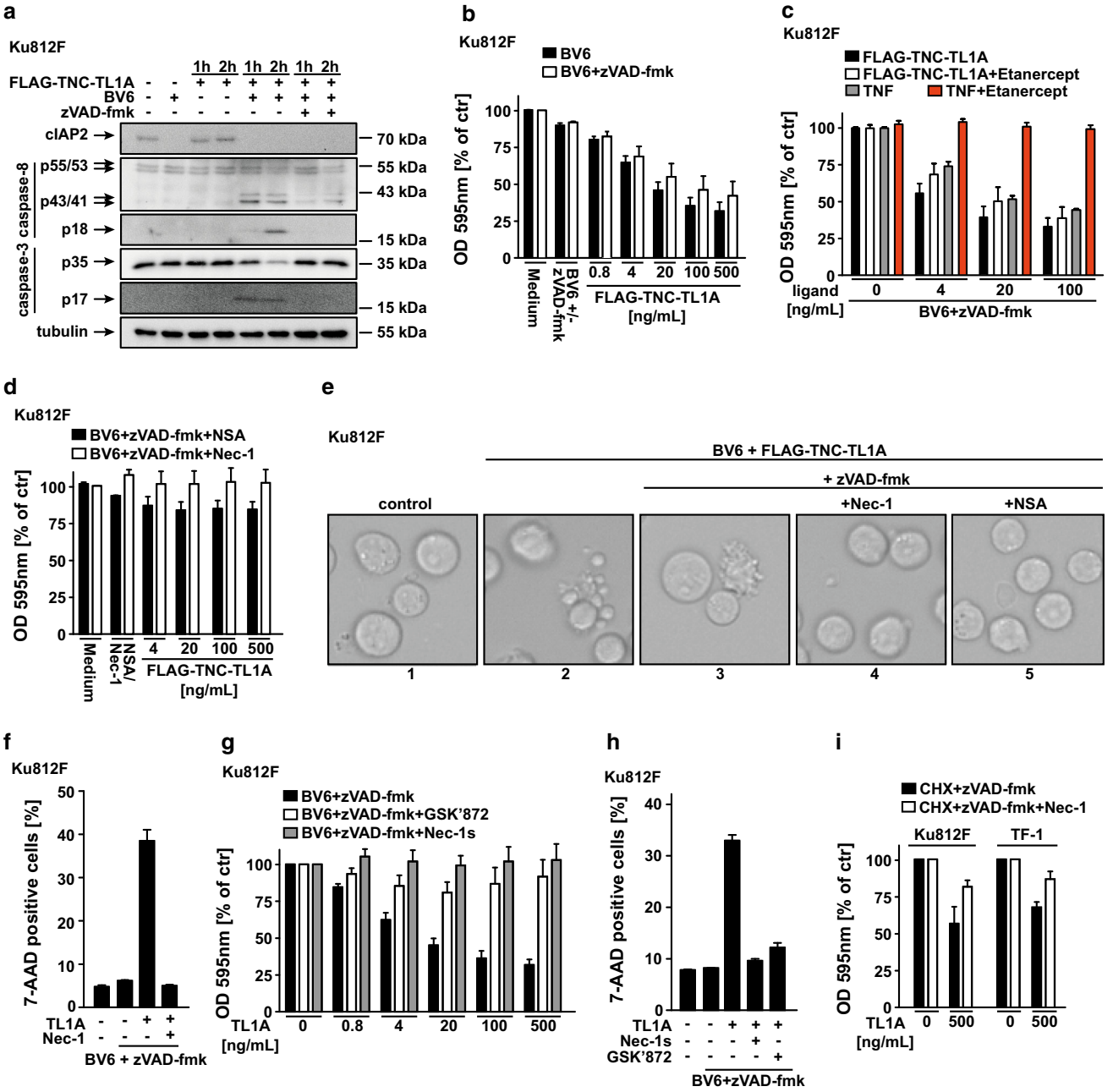

cIAP1/2-depleted Ku812F cells, the pan-caspase inhibitor zVAD-fmk efficiently blocked TL1A-induced caspase activation (Figs. 1f, 2a) but not cytotoxicity (Fig. 2b), thereby arguing against ongoing apoptotic cell death. Again, TL1A-triggered cytotoxic effects in BV6/zVAD-fmk-treated cells were not caused by autocrine TNF secretion (Fig. 2c). Beside caspase-dependent apoptosis, death receptors are also capable to trigger necroptosis, a caspase-independent cell death pathway that critically depends on RIP1/RIP3 [6, 7] and MLKL [20, 21]. Indeed, pharmacological inhibition of RIP1 using necrostatin-1 (Nec-1) and MLKL using necrosulfonamide (NSA) fully rescued BV6/zVAD-fmk-treated Ku812F cells from TL1A-induced cell death (Fig. 2d). These findings pointed to DR3-mediated necroptosis and were further substantiated by distinct changes in cell morphology. Compared to untreated controls, Ku812F cells challenged with TL1A in the presence of BV6 displayed typical apoptotic features such as cell shrinkage and plasma membrane blebbing (Fig. 2e, panel 1 and 2). Adding the caspase inhibitor zVAD-fmk changed the morphological pattern of TL1A-induced cell death in cIAP1/2-depleted cells. Plasma

membrane swelling and subsequent rupture (Fig. 2e, panel 3), indicative for necroptosis, was observable. Consistent with the protective role of Nec-1 and NSA in viability assays (Fig. 2d), both inhibitors abrogated TL1A-induced changes in cell morphology in the presence of BV6 and zVAD-fmk (Fig. 2e, panel 4 and 5). Accordingly, TL1A/BV6/zVAD-fmk treatment also induced loss of membrane integrity, as seen by significantly increased staining intensity for 7-AAD (Fig. 2f), a membrane impermeable DNA intercalating dye that is generally excluded from viable cells. In line with data from viability assays (Fig. 2d) and morphological analysis (Fig. 2e), Nec-1 was capable to prevent plasma membrane disintegration in cIAP1/2-depleted Ku812F cells in the presence of zVAD-fmk (Fig. 2f). The newer RIP1 inhibitor Nec-1s and the RIP3 inhibitor GSK'872 also efficiently protected Ku812F cells treated with TL1A/BV6/zVAD-fmk, as seen by viability assays (Fig. 2g) and preserved membrane integrity (Fig. 2h). In the presence of zVAD-fmk, not only SMAC mimetics but also CHX can act as a sensitizer for death ligand-induced necroptotic cell death. Accordingly, TL1A-induced cytotoxicity was detectable in CHX/zVAD-fmk-treated Ku812F and TF-1 cells (Fig. 2i) and significantly attenuated by Nec-1. Collectively, we observed that when caspase activation is blocked, DR3 can still exert cytotoxic effects in BV6 and/or CHX treated cells. Distinct changes in cellular morphology and full-blown protection granted by RIP1/RIP3 and/or MLKL inhibitors pointed to DR3-mediated necroptosis. To date, this cell death pathway has not been linked to DR3 signaling.

TL1A induces necrosome formation

Molecularly, necroptosis involves formation of a signaling complex (the "necrosome") containing RIP1/RIP3 as obligatory components for downstream MLKL activation. RIP3 and MLKL expression was detectable in both Ku812F and TF-1 cells, although RIP3 protein levels in the latter were significantly lower (Fig. 3a). In immunoprecipitation experiments, TL1A stimulation in the presence of BV6/zVAD-fmk triggered formation of a RIP1/RIP3 complex (Fig. 3b), which was inhibited when RIP1/RIP3 auto- and transphosphorylation was disturbed by Nec-1. The TL1A-induced formation of a RIP1/RIP3 complex was specific for DR3-mediated necroptosis, as absence of zVAD-fmk (allowing TL1A-triggered apoptotic cell death) expectedly resulted in reduced RIP3 levels (most likely through caspase-mediated RIP3 cleavage [31]) and abrogated RIP1/RIP3 interaction (Fig. 3c). As previously described for TNF-induced necroptosis [6], we also observed caspase-8 recruitment to RIP1 (Fig. 3d) when cIAP1/2 was depleted and caspase activation was blocked. In line with the requirement of RIP1 kinase activity for necrosome formation, Nec-1 treatment abrogated RIP1-caspase-8 interaction (Fig. 3e). Downstream of the RIP1/RIP3 complex, MLKL is the key effector molecule [20, 21]. Following phosphorylation and trimerization, MLKL locates to the cell plasma membrane, and finally executes necroptotic cell death [24]. Accordingly, in Ku812F cells treated with TL1A, BV6 and zVAD-fmk, phosphorylated MLKL migrating in SDS/PAGE at a position corresponding to the molecular weight of a trimer was detectable (Fig. 3f). This observation is in line with a previous study that reported SDS-stable phospho-MLKL aggregates [32]. In line with RIP3-mediated MLKL phosphorylation, trimeric phospho-MLKL was not detectable when assembly of the RIP1/RIP3 complex was disturbed by Nec-1 (Fig. 3f).

DR3-mediated necroptosis depends on HSP90 activity and RIP3

The critical role for RIP1, RIP3 and MLKL in DR3-mediated cytotoxicity when caspases are inactive was further substantiated by experiments using the heat shock protein 90 (HSP90) inhibitor 17-AAG. As observed previously [7, 33–36], 17-AAG decreased levels of RIP1, RIP3 and MLKL in Ku812F cells in a dose-dependent manner (Fig. 4a). In the presence of zVAD-fmk and BV6, reduction of RIP1/RIP3/MLKL levels blocked TL1A-induced necroptosis as seen by rescue of cell metabolic activity (Fig. 4b) and tremendously decreased 7-AAD positivity (Fig. 4c), an indicator for preserved plasma membrane integrity. Importantly and as expected, 17-AAG was not able to rescue Ku812F cells undergoing DR3-mediated apoptosis in the presence of TL1A and BV6 (Fig. 4d). Moreover, siRNA-mediated reduction of RIP3 in Ku812F cells diminished TL1A/BV6/zVAD-fmk-induced cell death (Fig. 4e). In sum, our data suggest that in the absence of caspase activity DR3 is capable to mediate cytotoxic effects via the "necroptotic" RIP1/RIP3/MLKL axis.

TAK1 kinase activity protects from DR3-mediated, RIP1 kinase-dependent necroptosis

Recently, a protective role for TGF-β-activated kinase 1 (TAK1) in TNF-triggered, RIP1-mediated apoptotic and necroptotic cell death has been reported [37, 38]. Briefly, cIAP1/2-dependent ubiquitination of RIP1 generates a scaffold for recruitment of TAK1 and the IκB kinase α/β (IKKα/β) complex to TNFR1, allowing IKKα/β activation via TAK1 [17]. IKKα/β phosphorylates RIP1 in complex I, thereby preventing RIP1 integration in complex IIb and abolishing RIP1-mediated apoptosis and necroptosis (reviewed in [39]). Therefore, in TNFR1 signaling not RIP1

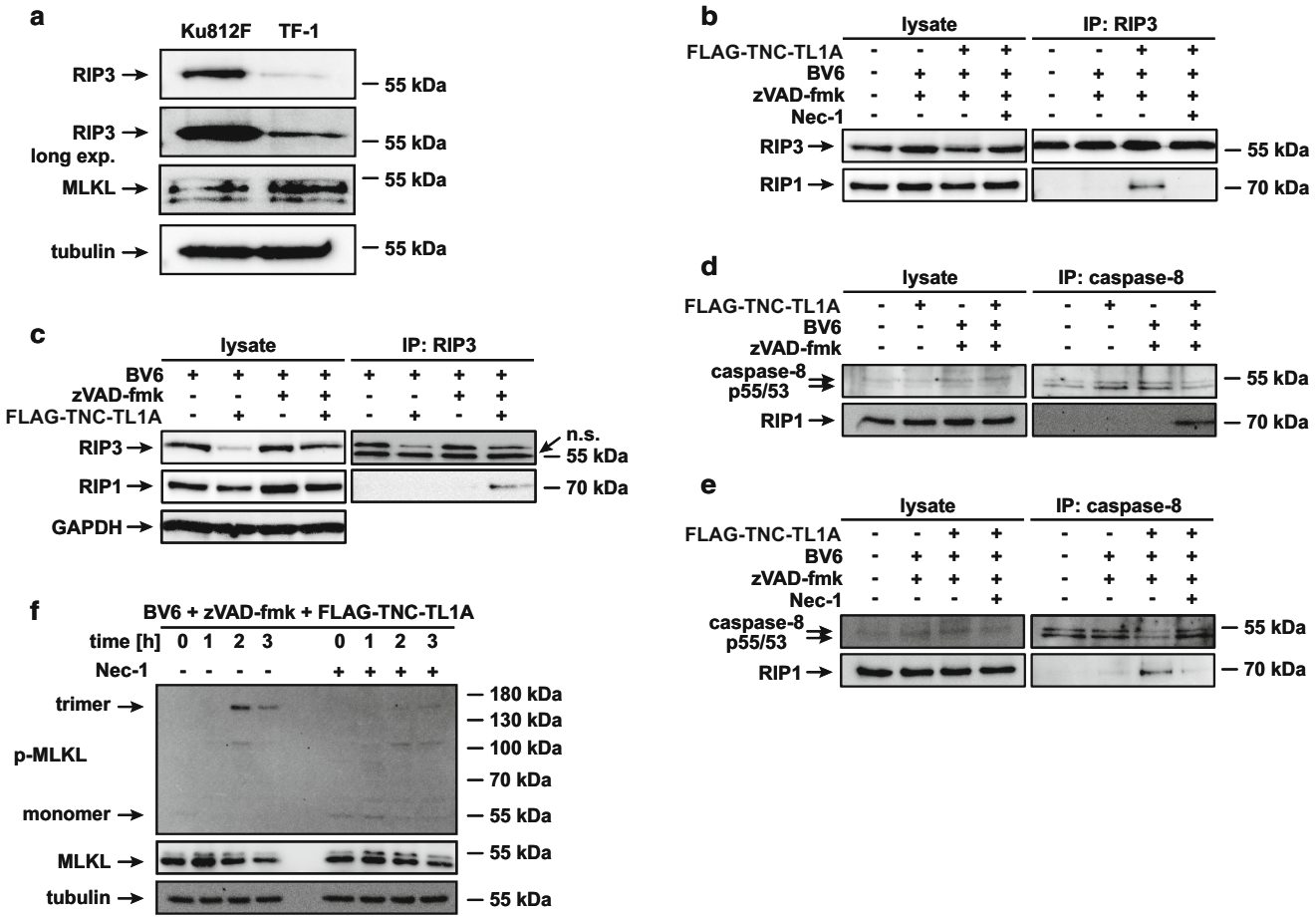

Fig. 3 TL1A induces necrosome formation. **a** RIP1, RIP3 and MLKL levels of Ku812F and TF-1 cells were analyzed using Western blotting. Detection of tubulin served as a loading control. **b**–**e** Ku812F cells were treated with BV6 (3 μM, 2 h), zVAD-fmk (100 μM, 1 h) in the presence and absence of Nec-1 (100 μM, 1 h), and subsequently challenged with FLAG-TNC-TL1A (400 ng/mL) for 2 h (**b**, **c**) or 1 h (**d**, **e**). After washing and cell lysis, immunoprecipitation was performed with antibodies specific for RIP3 (**b**, **c**) or caspase-8 (**d**, **e**). Immunoprecipitates were analyzed together with the corresponding lysates by Western blotting using antibodies specific for the indicated proteins. **f** Ku812F cells were treated with BV6 (3 μM, 2 h), zVAD-fmk (100 μM, 1 h) in the presence and absence of Nec-1 (100 μM, 1 h), and subsequently challenged with FLAG-TNC-TL1A (200 ng/mL) for the indicated periods of time. After washing and cell lysis, Western blot analyses were performed with antibodies specific for the indicated proteins. Detection of tubulin served as a loading control

ubiquitination per se, but ubiquitin-dependent recruitment of TAK1 and IKKα/β protects against RIP1-mediated cell death. We next assessed the role of TAK1 kinase activity in DR3-mediated RIP1 kinase-dependent necroptosis. In immunoprecipitation experiments using FLAG-tagged TL1A, we observed that BV6 but not the TAK1 inhibitor (5Z)-7-oxozeaenol (TAK1i) significantly reduced TL1A-induced RIP1 ubiquitination and allowed increased detection of non-ubiquitinated RIP1 (Fig. 5a). Functionally, TL1A displayed significant cytotoxicity in the presence of TAK1i, regardless whether caspase activation was blocked by zVAD-fmk or not (Fig. 5b). This is in good agreement with the capability of the RIP1-containing complex IIb to trigger both cell death modalities, caspase-dependent apoptosis and caspase-independent necroptosis. Accordingly, Nec-1s and NSA fully rescued Ku812F in the presence of TAK1i and zVAD-fmk. Interestingly, TF-1 cells underwent necroptotic cell death upon TL1A/CHX/zVAD-fmk treatment and apoptosis upon TL1A/BV6 stimulation (Figs. 1d, 2i), but we did not observe necroptosis induction using TL1A/BV6/zVAD-fmk (Fig. 5c) and TNF/BV6/zVAD-fmk (data not shown). This was most likely due to the inability of various SMAC mimetics to deplete cIAP1 in these cells (Fig. 5d). However, TL1A challenge in the presence of TAK1i and zVAD-fmk should result in necroptotic cell death irrespective of the RIP1 ubiquitination status. Indeed, TL1A/TAK1i/zVAD-fmk treatment exerted a cytotoxic effect that was abolished upon RIP1 or RIP3 inhibition using Nec-1s and GSK'872, respectively (Fig. 5e). Together our data suggest that, similar to TNFR1, also DR3-mediated RIP1-dependent necroptosis is controlled by TAK1 kinase activity.

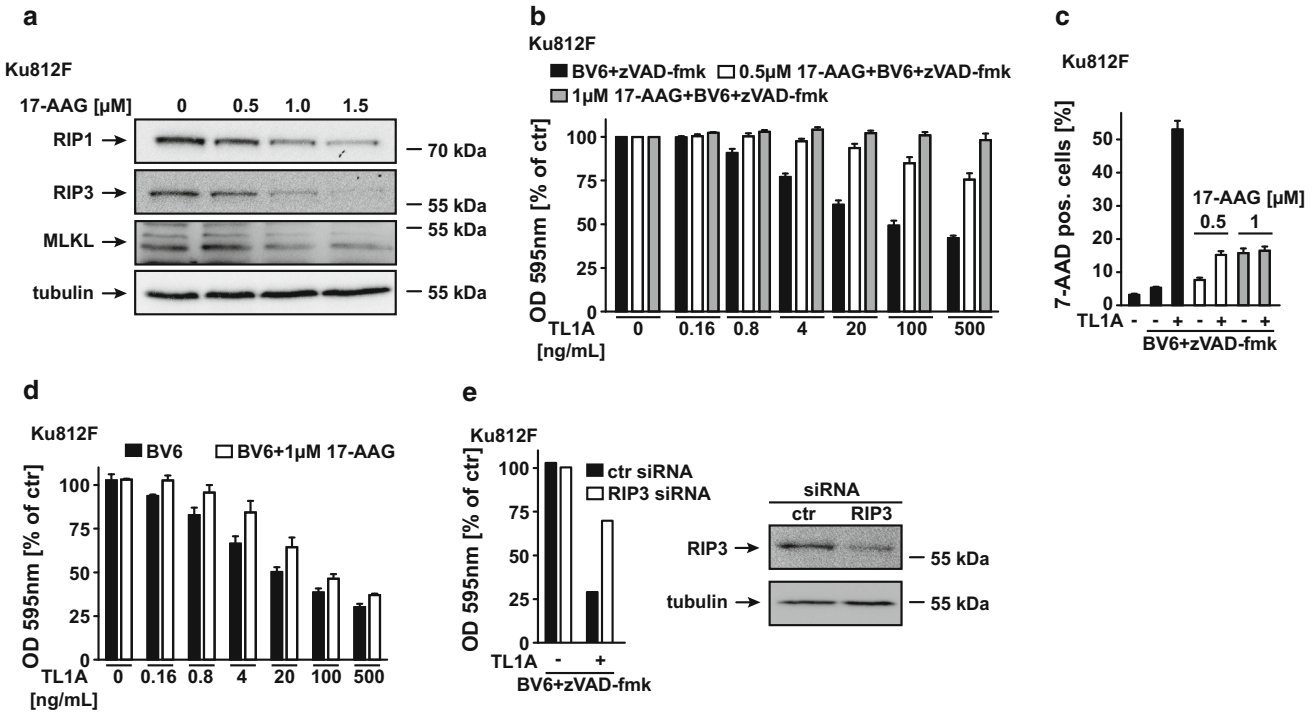

Fig. 4 DR3-mediated necroptosis depends on HSP90 activity and RIP3. **a** Ku812F cells were treated with indicated concentrations of the HSP90 inhibitor 17-AAG for 24 h. Subsequently, cellular levels of RIP1, RIP3 and MLKL were analyzed by Western blot with antibodies specific for indicated proteins. Detection of tubulin served as a loading control. **b** Ku812F cells were treated for 24 h with the indicated concentrations of 17-AAG. After washing, cells were treated with BV6 (3 μM, 2 h) and zVAD-fmk (100 μM, 1 h), and subsequently challenged with indicated concentrations of FLAG-TNC-TL1A. Viability was determined 4 h following stimulation by MTT staining. Values are mean ± SEM from three experiments. **c** Ku812F cells were treated with 17-AAG, BV6 and zVAD-fmk as described in **b** and subsequently challenged with FLAG-TNC-TL1A (200 ng/mL) for 4 h. Thereafter, loss of membrane integrity was analyzed by flow cytometry using 7-AAD staining. Values are mean ± SEM from three experiments. **d** Ku812F cells were treated for 24 h with 17-AAG (1 μM). After washing, cells were treated with BV6 (3 μM, 2 h), and subsequently challenged with FLAG-TNC-TL1A. Viability was determined 4 h following stimulation by MTT staining. Values are mean ± SEM from three experiments. **e** Ku812F cells were treated with RIP3-specific or non-targeting siRNA (control, ctr) as described in "Materials and methods". 48 h after siRNA electroporation, cells were treated with BV6 (3 μM, 2 h) and zVAD-fmk (100 μM, 1 h) and subsequently challenged with 500 ng/mL FLAG-TNC-TL1A for 4 h. Knockdown efficiency was assessed by Western blotting, detection of tubulin served as loading control. Data shown are representative of two experiments performed

DR3-mediated necroptosis is accompanied but not caused by ROS production

A number of studies provided evidence for the production of reactive oxygen species (ROS) during necroptosis [5, 24, 37, 40–43]. Their functional relevance, however, is controversially discussed, especially in TNF-induced necroptotic cell death [44, 45]. In BV6/zVAD-fmk-treated Ku812F cells, TL1A stimulation significantly increased cellular ROS levels (Fig. 6a). Rescue from TL1A-induced necroptosis using Nec-1 expectedly abolished ROS production (Fig. 6b). Although in Ku812F cells H_2O_2-derived ROS were efficiently scavenged by butylated hydroxyanisole (BHA) (Fig. 6c), BHA failed to protected Ku812F cells from TL1A- or TNF-induced necroptotic cell death (Fig. 6d). To further rule out the inefficient ROS scavenging of BHA, we also addressed the effects of ROS neutralization on TNF-induced necroptosis in the L929 fibrosarcoma cell line. In cIAP1/2-depleted L929 cells, TNF induces ROS-dependent necroptosis in the absence of caspase or protein synthesis inhibitors [37]. In this cellular model, BHA and Nec-1 were equally protective against TNF-induced necroptosis (Fig. 6e, f). Taken together, these data suggest that DR3-mediated necroptosis is accompanied by but not depending on ROS production. But admittedly, the requirement of ROS for necroptosis may depend on the cellular context.

Discussion

The morphological distinct features of necrosis were already recognized by Rudolf Virchow in the mid-nineteenth century and it soon became obvious that necrosis can either be a cause or a consequence of disease.

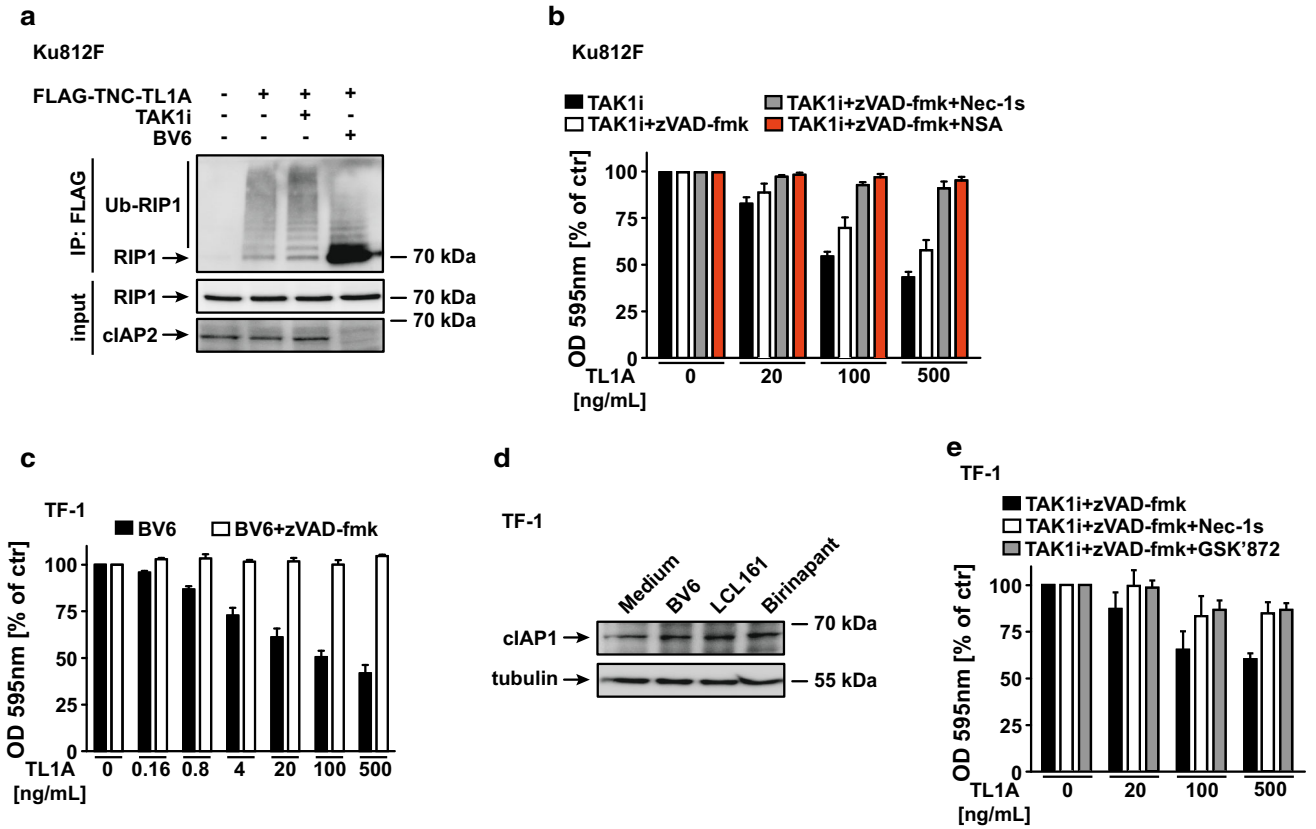

Fig. 5 TAK1 kinase activity protects cells from RIP1-mediated cell death. **a** Ku812F cells were treated with BV6 (3 μM) or the TAK1-inhibitor (TAK1i) (5Z)-7-oxozeaenol (0.8 μM) for 1 h, and subsequently challenged with 1 μg/mL FLAG-TNC-TL1A for 10 min. After washing and cell lysis, immunoprecipitation was performed using anti-FLAG antibodies. Immunoprecipitates were analyzed together with the corresponding lysates by Western blotting using antibodies specific for the indicated proteins. **b** Ku812F cells were treated with TAK1i (0.8 μM), zVAD-fmk (100 μM), Nec-1s (30 μM) and NSA (25 μM) for 1 h, and subsequently challenged with FLAG-TNC-TL1A. Viability was determined 4 h following stimulation by MTT staining. Values are mean ± SEM from three experiments. **c** TF-1 cells were treated with BV6 (10 μM, 2 h) and zVAD-fmk (100 μM, 1 h), and subsequently challenged with FLAG-TNC-TL1A. 18 h after stimulation, viability was determined by MTT staining. Values are mean ± SEM from three experiments. **d** TF-1 cells were treated with 10 μM of the SMAC mimetics BV6, LCL161 or Birinapant for 2 h. Thereafter, cIAP1 levels in cell lysates were determined using Western blotting. Detection of tubulin served as loading control. **e** TF-1 cells were treated with TAK1i (3 μM), zVAD-fmk (100 μM), Nec-1s (30 μM) and GSK'872 (8 μM) for 1 h. Subsequently, cells were challenged with FLAG-TNC-TL1A. Viability was determined 4 h following stimulation by MTT staining. Values are mean ± SEM from three experiments

However, the apparently "unregulated" nature of this cell death modality gave little hope for therapeutic intervention. This drastically changed upon realizing that some forms of necrotic cell death (e.g., necroptosis) are driven by distinct, targetable molecular pathways and are contributors to a variety of pathophysiological processes, such as ischemic injury, infections, chronic inflammation and cancer [2]. To date, the network of regulated, non-apoptotic cell death pathways has grown considerably [46]. The meanwhile profound understanding of the molecular mechanisms underlying regulated necrosis together with the availability of necroptosis inhibitors brought up novel therapeutic options and small molecules targeting components of the necroptotic machinery are emerging as potential therapeutic agents [47].

In many pathological conditions, however, it remains unclear what actually triggered necroptosis. In vitro studies highlighted death receptors, especially TNFR1, as primary inducers of necroptotic cell death. However, deficiency in TNFR1 did not protect mice in models of renal ischemia/reperfusion injury [48], suggesting that other (death) receptors and/or signals could be involved to induce necroptosis. Beside TNFR1, the death receptors thus far recognized for necroptosis induction include the TRAIL death receptors TRAILR1 and TRAILR2 as well as CD95 [8].

With DR3, our study identifies another death receptor capable to trigger a regulated form of necrosis. According to our findings, DR3- and TNFR1-mediated necroptosis share several features, as both (a) require blocked caspase activation along with cIAP1/2 depletion (Fig. 2b) or TAK1/IKKα/β inhibition (Fig. 5); (b) involve a RIP1/RIP3 containing necrosome and MLKL as downstream effector (Fig. 3); (c) depend on HSP90 to ensure stability of RIP1/RIP3 and MLKL (Fig. 4) and (d) trigger ROS production

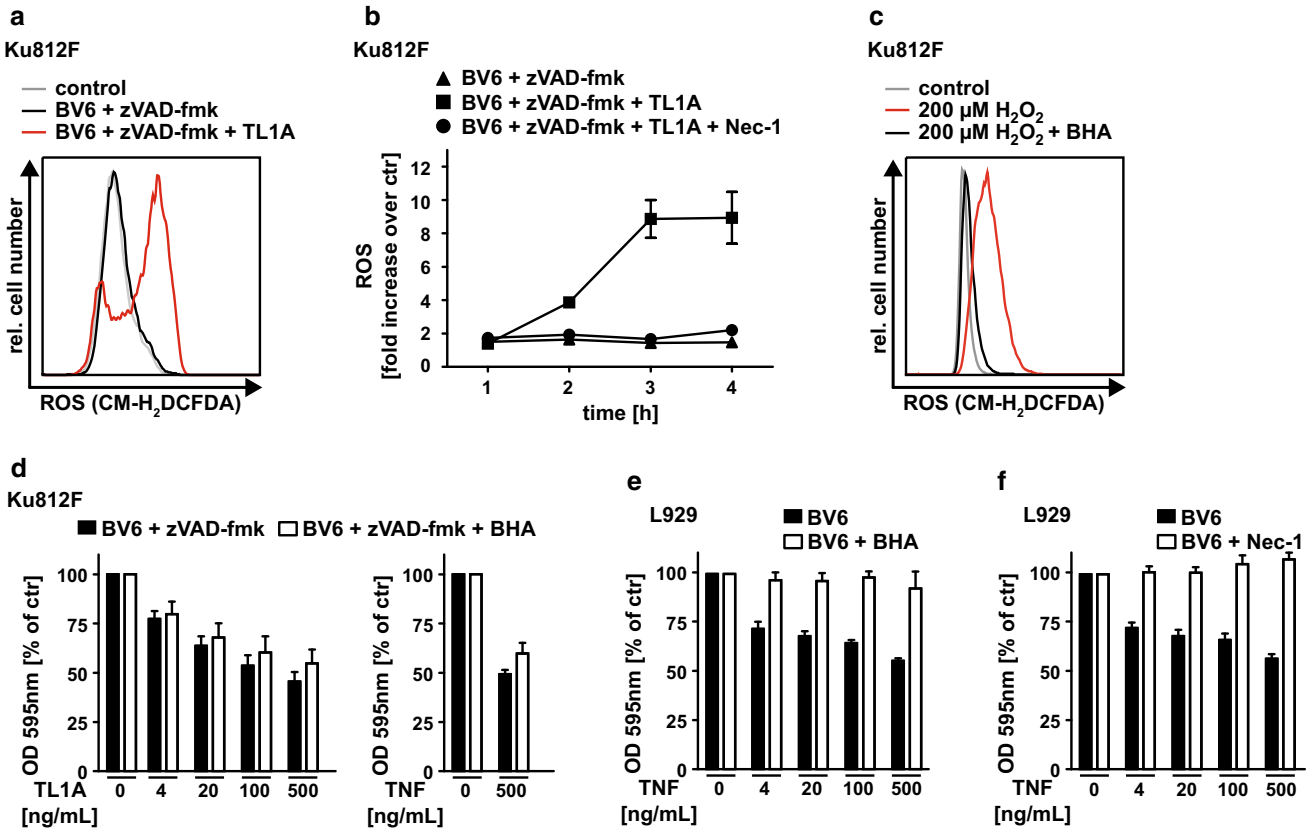

Fig. 6 DR3-mediated necroptosis is accompanied but not caused by ROS production. **a** Ku812F cells were treated with BV6 (3 µM, 2 h) and zVAD-fmk (100 µM, 1 h) followed by challenge with FLAG-TNC-TL1A (200 ng/mL). 90 min after stimulation, CM-H_2DCFDA (5 µM) was added and incubated at 37 °C for 30 min. ROS generation was measured using flow cytometry. Data shown are representative of three experiments performed. **b** Ku812F cells were treated with BV6 and zVAD-fmk as described above, and subsequently challenged with FLAG-TNC-TL1A (200 ng/mL) for the indicated periods of time (*black circles* and *black squares*) or left without FLAG-TNC-TL1A addition (*black triangles*). Nec-1 (100 µM, *black circles*) was added 1 h before stimulation. ROS increase was calculated by division of the mean fluorescence intensity (MFI) of treated cells by MFI of untreated cells. Shown are mean values ± SEM from three experiments. **c** Ku812 cells were challenged with 200 µM H_2O_2 in the presence and absence of BHA (100 µM, 1 h). **d** Ku812F cells were treated with BV6 (3 µM, 2 h), zVAD-fmk (100 µM, 1 h) and BHA (100 µM, 1 h) followed by stimulation with FLAG-TNC-TL1A (*left panel*) or TNF (*right panel*) with the indicated concentrations for 4 h. Viability was subsequently determined by MTT staining. Values are mean ± SEM from three experiments. **e–f** L929 cells were treated with BV6 (2.5 µM, 2 h), BHA (100 µM, 1 h) and Nec-1 (100 µM, 1 h). Subsequently, cells were challenged with indicated concentrations of TNF for 18 h. Viability was determined by MTT staining. Values are mean ± SEM from three experiments

(Fig. 6). It is still a matter of debate (reviewed in [49]) whether ROS are critical regulators necroptosis [7, 44] or a by-product generated in the course of this cell death mechanism [45]. Although our data do not support a major role of ROS in DR3-mediated necroptosis (Fig. 6), we can admittedly not fully exclude cell line specific effects.

Despite the mechanistic similarities in TNFR1- and DR3-mediated necroptosis and the structural relatedness of these two death receptors, the fundamentally different distribution of TNFR1 and DR3 across cell types is worth mentioning. Whereas TNFR1 is almost ubiquitously expressed, DR3 is found predominantly on lymphocytes, including several B and T cell subsets (e.g., activated $CD4^+/CD8^+$ T cells, regulatory T cells) and innate lymphoid cells (ILCs) [26]. Beside immune cells, DR3 expression has also been reported on interstitial vascular endothelial cells in the human kidney [50], an organ in which necroptosis plays a major role in ischemia/reperfusion injury [51]. A role for DR3-mediated necroptosis in these cells or tissues has to date not been addressed but is worth investigating. Inflammatory processes commonly involve a complex mixture of TNF family ligands, e.g., TNF-like weak inducer of apoptosis (TWEAK), TL1A and TNF itself. Moreover, most cell types harbor receptors for various TNF ligands on their surface. As TNF receptors commonly share a cytoplasmic pool of proteins for signal transduction, simultaneous or sequential activation of different TNF receptors can alter the accessibility of adapter molecules, and thereby fundamentally shift the resulting cellular response ("receptor crosstalk"). For example, TNFR2 activation depletes TRAF2–cIAP complexes from the cytoplasmic pool, thereby switching subsequent

TNFR1 signaling from inflammation to apoptosis [52]. Notably, TRAF2–cIAP complexes are also important necroptosis suppressors [53]. TRAF2–cIAP depletion via the TWEAK/Fn14 axis essentially mimics the effect of SMAC mimetics and boosts TRAIL- and CD95L-induced necroptosis [54]. It is therefore conceivable that conditions allowing necroptotic cell death not only exist in in vitro settings with exogenous additions of SMAC mimetics and/or pharmacological caspase inhibitors, but potentially also under inflammatory conditions.

In sum, by identifying DR3 as a novel necroptosis-inducing death receptor our study extends our understanding of the TL1A–DR3 signaling axis and adds another player to the plethora of necrosome triggers [55].

Acknowledgments ME is supported by grants from Deutsche Forschungsgemeinschaft (DFG Grant EH 465/2-1), the Roggenbuck Stiftung and the Medical Faculty of the University of Regensburg ("ReForM-B").

References

1. Hanahan D, Weinberg RA (2011) Hallmarks of cancer: the next generation. Cell 144(5):646–674. doi:10.1016/j.cell.2011.02.013
2. Linkermann A, Green DR (2014) Necroptosis. N Engl J Med 370(5):455–465. doi:10.1056/NEJMra1310050
3. Steller H (1995) Mechanisms and genes of cellular suicide. Science 267(5203):1445–1449. doi:10.1126/science.7878463
4. Ashkenazi A, Salvesen G (2014) Regulated cell death: signaling and mechanisms. Annu Rev Cell Dev Biol 30:337–356. doi:10.1146/annurev-cellbio-100913-013226
5. Zhang DW, Shao J, Lin J, Zhang N, Lu BJ, Lin SC, Dong MQ, Han J (2009) RIP3, an energy metabolism regulator that switches TNF-induced cell death from apoptosis to necrosis. Science 325(5938):332–336. doi:10.1126/science.1172308
6. He S, Wang L, Miao L, Wang T, Du F, Zhao L, Wang X (2009) Receptor interacting protein kinase-3 determines cellular necrotic response to TNF-alpha. Cell 137(6):1100–1111. doi:10.1016/j.cell.2009.05.021
7. Cho YS, Challa S, Moquin D, Genga R, Ray TD, Guildford M, Chan FK (2009) Phosphorylation-driven assembly of the RIP1–RIP3 complex regulates programmed necrosis and virus-induced inflammation. Cell 137(6):1112–1123. doi:10.1016/j.cell.2009.05.037
8. Holler N, Zaru R, Micheau O, Thome M, Attinger A, Valitutti S, Bodmer JL, Schneider P, Seed B, Tschopp J (2000) Fas triggers an alternative, caspase-8-independent cell death pathway using the kinase RIP as effector molecule. Nat Immunol 1(6):489–495. doi:10.1038/82732
9. Laster SM, Wood JG, Gooding LR (1988) Tumor necrosis factor can induce both apoptic and necrotic forms of cell lysis. J Immunol 141(8):2629–2634
10. Micheau O, Tschopp J (2003) Induction of TNF receptor I-mediated apoptosis via two sequential signaling complexes. Cell 114(2):181–190. doi:10.1016/S0092-8674(03)00521-X
11. Dillon CP, Weinlich R, Rodriguez DA, Cripps JG, Quarato G, Gurung P, Verbist KC, Brewer TL, Llambi F, Gong YN, Janke LJ, Kelliher MA, Kanneganti TD, Green DR (2014) RIPK1 blocks early postnatal lethality mediated by caspase-8 and RIPK3. Cell 157(5):1189–1202. doi:10.1016/j.cell.2014.04.018
12. Bertrand MJ, Milutinovic S, Dickson KM, Ho WC, Boudreault A, Durkin J, Gillard JW, Jaquith JB, Morris SJ, Barker PA (2008) cIAP1 and cIAP2 facilitate cancer cell survival by functioning as E3 ligases that promote RIP1 ubiquitination. Mol Cell 30(6):689–700. doi:10.1016/j.molcel.2008.05.014
13. Varfolomeev E, Goncharov T, Fedorova AV, Dynek JN, Zobel K, Deshayes K, Fairbrother WJ, Vucic D (2008) c-IAP1 and c-IAP2 are critical mediators of tumor necrosis factor alpha (TNFalpha)-induced NF-kappaB activation. J Biol Chem 283(36):24295–24299. doi:10.1074/jbc.C800128200
14. Mahoney DJ, Cheung HH, Mrad RL, Plenchette S, Simard C, Enwere E, Arora V, Mak TW, Lacasse EC, Waring J, Korneluk RG (2008) Both cIAP1 and cIAP2 regulate TNFalpha-mediated NF-kappaB activation. Proc Natl Acad Sci USA 105(33):11778–11783. doi:10.1073/pnas.0711122105
15. Wang L, Du F, Wang X (2008) TNF-alpha induces two distinct caspase-8 activation pathways. Cell 133(4):693–703. doi:10.1016/j.cell.2008.03.036
16. O'Donnell MA, Legarda-Addison D, Skountzos P, Yeh WC, Ting AT (2007) Ubiquitination of RIP1 regulates an NF-kappaB-independent cell-death switch in TNF signaling. Curr Biol 17(5):418–424. doi:10.1016/j.cub.2007.01.027
17. Dondelinger Y, Jouan-Lanhouet S, Divert T, Theatre E, Bertin J, Gough PJ, Giansanti P, Heck AJ, Dejardin E, Vandenabeele P, Bertrand MJ (2015) NF-kappaB-independent role of IKKalpha/IKKbeta in preventing RIPK1 kinase-dependent apoptotic and necroptotic cell death during TNF signaling. Mol Cell 60(1):63–76. doi:10.1016/j.molcel.2015.07.032
18. Li J, McQuade T, Siemer AB, Napetschnig J, Moriwaki K, Hsiao YS, Damko E, Moquin D, Walz T, McDermott A, Chan FK, Wu H (2012) The RIP1/RIP3 necrosome forms a functional amyloid signaling complex required for programmed necrosis. Cell 150(2):339–350. doi:10.1016/j.cell.2012.06.019
19. Degterev A, Hitomi J, Germscheid M, Ch'en IL, Korkina O, Teng X, Abbott D, Cuny GD, Yuan C, Wagner G, Hedrick SM, Gerber SA, Lugovskoy A, Yuan J (2008) Identification of RIP1 kinase as a specific cellular target of necrostatins. Nat Chem Biol 4(5):313–321. doi:10.1038/nchembio.83
20. Zhao J, Jitkaew S, Cai Z, Choksi S, Li Q, Luo J, Liu ZG (2012) Mixed lineage kinase domain-like is a key receptor interacting protein 3 downstream component of TNF-induced necrosis. Proc Natl Acad Sci USA 109(14):5322–5327. doi:10.1073/pnas.1200012109
21. Sun L, Wang H, Wang Z, He S, Chen S, Liao D, Wang L, Yan J, Liu W, Lei X, Wang X (2012) Mixed lineage kinase domain-like protein mediates necrosis signaling downstream of RIP3 kinase. Cell 148(1–2):213–227. doi:10.1016/j.cell.2011.11.031
22. Murphy JM, Czabotar PE, Hildebrand JM, Lucet IS, Zhang JG, Alvarez-Diaz S, Lewis R, Lalaoui N, Metcalf D, Webb AI, Young SN, Varghese LN, Tannahill GM, Hatchell EC, Majewski IJ, Okamoto T, Dobson RC, Hilton DJ, Babon JJ, Nicola NA, Strasser A, Silke J, Alexander WS (2013) The pseudokinase MLKL mediates necroptosis via a molecular switch mechanism. Immunity 39(3):443–453. doi:10.1016/j.immuni.2013.06.018
23. Rodriguez DA, Weinlich R, Brown S, Guy C, Fitzgerald P, Dillon CP, Oberst A, Quarato G, Low J, Cripps JG, Chen T, Green DR (2016) Characterization of RIPK3-mediated phosphorylation of the activation loop of MLKL during necroptosis. Cell Death Differ 23(1):76–88. doi:10.1038/cdd.2015.70
24. Cai Z, Jitkaew S, Zhao J, Chiang HC, Choksi S, Liu J, Ward Y, Wu LG, Liu ZG (2014) Plasma membrane translocation of trimerized MLKL protein is required for TNF-induced necroptosis. Nat Cell Biol 16(1):55–65. doi:10.1038/ncb2883
25. Migone TS, Zhang J, Luo X, Zhuang L, Chen C, Hu B, Hong JS, Perry JW, Chen SF, Zhou JX, Cho YH, Ullrich S, Kanakaraj P, Carrell J, Boyd E, Olsen HS, Hu G, Pukac L, Liu D, Ni J, Kim S,

Gentz R, Feng P, Moore PA, Ruben SM, Wei P (2002) TL1A is a TNF-like ligand for DR3 and TR6/DcR3 and functions as a T cell costimulator. Immunity 16(3):479–492. doi:10.1016/S1074-7613(02)00283-2
26. Richard AC, Ferdinand JR, Meylan F, Hayes ET, Gabay O, Siegel RM (2015) The TNF-family cytokine TL1A: from lymphocyte costimulator to disease co-conspirator. J Leukoc Biol 98(3):333–345. doi:10.1189/jlb.3RI0315-095R
27. Wen L, Zhuang L, Luo X, Wei P (2003) TL1A-induced NF-kappaB activation and c-IAP2 production prevent DR3-mediated apoptosis in TF-1 cells. J Biol Chem 278(40):39251–39258. doi:10.1074/jbc.M305833200
28. Chinnaiyan AM, O'Rourke K, Yu GL, Lyons RH, Garg M, Duan DR, Xing L, Gentz R, Ni J, Dixit VM (1996) Signal transduction by DR3, a death domain-containing receptor related to TNFR-1 and CD95. Science 274(5289):990–992. doi:10.1126/science.274.5289.990
29. Bittner S, Knoll G, Fullsack S, Kurz M, Wajant H, Ehrenschwender M (2016) Soluble TL1A is sufficient for activation of death receptor 3. FEBS J 283(2):323–336. doi:10.1111/febs.13576
30. Ehrenschwender M, Bittner S, Seibold K, Wajant H (2014) XIAP-targeting drugs re-sensitize PIK3CA-mutated colorectal cancer cells for death receptor-induced apoptosis. Cell Death Dis 5:e1570. doi:10.1038/cddis.2014.534
31. Feng S, Yang Y, Mei Y, Ma L, Zhu DE, Hoti N, Castanares M, Wu M (2007) Cleavage of RIP3 inactivates its caspase-independent apoptosis pathway by removal of kinase domain. Cell Signal 19(10):2056–2067. doi:10.1016/j.cellsig.2007.05.016
32. Yoon S, Bogdanov K, Kovalenko A, Wallach D (2016) Necroptosis is preceded by nuclear translocation of the signaling proteins that induce it. Cell Death Differ 23(2):253–260. doi:10.1038/cdd.2015.92
33. Li D, Xu T, Cao Y, Wang H, Li L, Chen S, Wang X, Shen Z (2015) A cytosolic heat shock protein 90 and cochaperone CDC37 complex is required for RIP3 activation during necroptosis. Proc Natl Acad Sci USA 112(16):5017–5022. doi:10.1073/pnas.1505244112
34. Vanden Berghe T, Kalai M, van Loo G, Declercq W, Vandenabeele P (2003) Disruption of HSP90 function reverts tumor necrosis factor-induced necrosis to apoptosis. J Biol Chem 278(8):5622–5629. doi:10.1074/jbc.M208925200
35. Fearns C, Pan Q, Mathison JC, Chuang TH (2006) Triad3A regulates ubiquitination and proteasomal degradation of RIP1 following disruption of Hsp90 binding. J Biol Chem 281(45):34592–34600. doi:10.1074/jbc.M604019200
36. Lewis J, Devin A, Miller A, Lin Y, Rodriguez Y, Neckers L, Liu ZG (2000) Disruption of hsp90 function results in degradation of the death domain kinase, receptor-interacting protein (RIP), and blockage of tumor necrosis factor-induced nuclear factor-kappaB activation. J Biol Chem 275(14):10519–10526. doi:10.1074/jbc.275.14.10519
37. Vanlangenakker N, Vanden Berghe T, Bogaert P, Laukens B, Zobel K, Deshayes K, Vucic D, Fulda S, Vandenabeele P, Bertrand MJ (2011) cIAP1 and TAK1 protect cells from TNF-induced necrosis by preventing RIP1/RIP3-dependent reactive oxygen species production. Cell Death Differ 18(4):656–665. doi:10.1038/cdd.2010.138
38. Dondelinger Y, Aguileta MA, Goossens V, Dubuisson C, Grootjans S, Dejardin E, Vandenabeele P, Bertrand MJ (2013) RIPK3 contributes to TNFR1-mediated RIPK1 kinase-dependent apoptosis in conditions of cIAP1/2 depletion or TAK1 kinase inhibition. Cell Death Differ 20(10):1381–1392. doi:10.1038/cdd.2013.94
39. Ting AT, Bertrand MJ (2016) More to life than NF-kappaB in TNFR1 signaling. Trends Immunol 37(8):535–545. doi:10.1016/j.it.2016.06.002
40. Vanden Berghe T, Vanlangenakker N, Parthoens E, Deckers W, Devos M, Festjens N, Guerin CJ, Brunk UT, Declercq W, Vandenabeele P (2010) Necroptosis, necrosis and secondary necrosis converge on similar cellular disintegration features. Cell Death Differ 17(6):922–930. doi:10.1038/cdd.2009.184
41. Shulga N, Pastorino JG (2012) GRIM-19-mediated translocation of STAT3 to mitochondria is necessary for TNF-induced necroptosis. J Cell Sci 125(Pt 12):2995–3003. doi:10.1242/jcs.103093
42. Shindo R, Kakehashi H, Okumura K, Kumagai Y, Nakano H (2013) Critical contribution of oxidative stress to TNFalpha-induced necroptosis downstream of RIPK1 activation. Biochem Biophys Res Commun 436(2):212–216. doi:10.1016/j.bbrc.2013.05.075
43. Kim YS, Morgan MJ, Choksi S, Liu ZG (2007) TNF-induced activation of the Nox1 NADPH oxidase and its role in the induction of necrotic cell death. Mol Cell 26(5):675–687. doi:10.1016/j.molcel.2007.04.021
44. Schenk B, Fulda S (2015) Reactive oxygen species regulate Smac mimetic/TNFalpha-induced necroptotic signaling and cell death. Oncogene 34(47):5796–5806. doi:10.1038/onc.2015.35
45. Tait SW, Oberst A, Quarato G, Milasta S, Haller M, Wang R, Karvela M, Ichim G, Yatim N, Albert ML, Kidd G, Wakefield R, Frase S, Krautwald S, Linkermann A, Green DR (2013) Widespread mitochondrial depletion via mitophagy does not compromise necroptosis. Cell Rep 5(4):878–885. doi:10.1016/j.celrep.2013.10.034
46. Vanden Berghe T, Linkermann A, Jouan-Lanhouet S, Walczak H, Vandenabeele P (2014) Regulated necrosis: the expanding network of non-apoptotic cell death pathways. Nat Rev Mol Cell Biol 15(2):135–147. doi:10.1038/nrm3737
47. Degterev A, Linkermann A (2016) Generation of small molecules to interfere with regulated necrosis. Cell Mol Life Sci 73(11–12):2251–2267. doi:10.1007/s00018-016-2198-x
48. Burne MJ, Elghandour A, Haq M, Saba SR, Norman J, Condon T, Bennett F, Rabb H (2001) IL-1 and TNF independent pathways mediate ICAM-1/VCAM-1 up-regulation in ischemia reperfusion injury. J Leukoc Biol 70(2):192–198
49. Fulda S (2016) Regulation of necroptosis signaling and cell death by reactive oxygen species. Biol Chem 397(7):657–660. doi:10.1515/hsz-2016-0102
50. Wang J, Al-Lamki RS, Zhu X, Liu H, Pober JS, Bradley JR (2014) TL1-A can engage death receptor-3 and activate NF-kappa B in endothelial cells. BMC Nephrol 15(1):1–10. doi:10.1186/1471-2369-15-178
51. Linkermann A, Bräsen JH, Himmerkus N, Liu S, Huber TB, Kunzendorf U, Krautwald S (2012) Rip1 (receptor-interacting protein kinase 1) mediates necroptosis and contributes to renal ischemia/reperfusion injury. Kidney Int 81(8):751–761. doi:10.1038/ki.2011.450
52. Fotin-Mleczek M, Henkler F, Samel D, Reichwein M, Hausser A, Parmryd I, Scheurich P, Schmid JA, Wajant H (2002) Apoptotic crosstalk of TNF receptors: TNF-R2-induces depletion of TRAF2 and IAP proteins and accelerates TNF-R1-dependent activation of caspase-8. J Cell Sci 115(Pt 13):2757–2770
53. Petersen SL, Chen TT, Lawrence DA, Marsters SA, Gonzalvez F, Ashkenazi A (2015) TRAF2 is a biologically important necroptosis suppressor. Cell Death Differ 22(11):1846–1857. doi:10.1038/cdd.2015.35
54. Karl I, Jossberger-Werner M, Schmidt N, Horn S, Goebeler M, Leverkus M, Wajant H, Giner T (2014) TRAF2 inhibits TRAIL- and CD95L-induced apoptosis and necroptosis. Cell Death Dis 5:e1444. doi:10.1038/cddis.2014.404
55. Vanden Berghe T, Hassannia B, Vandenabeele P (2016) An outline of necrosome triggers. Cell Mol Life Sci 73(11–12):2137–2152. doi:10.1007/s00018-016-2189-y